

# FORCE FIELDS WITHIN MICHELL-LIKE CANTILEVERS TRANSMITTING A POINT LOAD TO A STRAIGHT SUPPORT

Cezary Graczykowski<sup>1</sup> and Tomasz Lewiński<sup>2</sup>

<sup>1</sup>*Institute of Fundamental Technological Research, Polish Academy of Sciences, Świętokrzyska 21, 00-049 Warszawa, Poland*

<sup>2</sup>*Institute of Structural Mechanics, Faculty of Civil Engineering, Warsaw University of Technology, al. Armii Ludowej 16, 00-637 Warsaw, Poland*

**Abstract:** The paper concerns distribution of the force fields within Michell cantilevers supported on a segment of a straight line. The allowable yield stresses for tension and compression are not necessarily equal. The paper puts emphasis on checking the final results for the optimal weight by computing the weight in two manners: as a virtual work or, alternatively, by finding the force fields, the density of fibres and then by summing up the weights of all the parts of the optimal cantilever, i.e. the weights of the reinforcing bars and the weights of all the fibrous domains. If this duality gap vanishes, the solution is correct.

**Keywords:** Michell-like cantilevers, minimum weight problem, topology optimization.

## 1. INTRODUCTION

The Michell problem can be expressed in terms of average stress fields as a minimum weight problem or in terms of displacements as a maximization problem, see Strang and Kohn (1983). The latter problem can be interpreted as an equilibrium problem of a body with locking, see Golay and Seppacher (2001), Lewiński and Telega (2001). The known analytical solutions were found just within the framework of this formulation. In particular, the Michell (1904) cantilever supported on a circle (see Hemp, 1973) was found by guessing the kinematically admissible virtual displacements realizing the optimality conditions  $\varepsilon_I = 1$ ,  $\varepsilon_{II} = -1$  concerning the principal values of the tensor of virtual strains in the problem in which the allowable yield local stresses for tension ( $\sigma_T$ ) and compression ( $\sigma_C$ ) are equal:  $\sigma_T = \sigma_C$ . The weight of the optimal cantilever is equal up to a factor to the value of the work of the point load applied to a joint on the displacement of this joint. Let us emphasize here

that this displacement is finite since the reinforcing bars connected at this joint transmit the point load thus eliminating possible stress singularities. We see that having the virtual displacements the computation of the weight becomes straightforward. On the other hand, computation of this weight within the average stress-based formulation is more complex. Note that none of the available exact solutions to the Michell problem was solved with using the stress-based formulation. This would require finding the minimizer of the weight (expressed in terms of average stresses) among all candidates which are statically admissible. This is not an easy task, since this set is affine and hard to parameterize. It is easier to recover the average stress fields upon finding the Hencky net, the latter being featured by the displacement-based optimality criteria (see Hemp, 1973, sec. 4.3). The average stresses found this manner should be correlated with longitudinal forces in the reinforcing bars. For instance, the weight of the cantilever supported on a circle is equal to the sum of weights of the reinforcing bars and the fibrous interior. The weight computed this manner is exactly equal to the virtual work of the applied point load. The relevant analytical proof has been only recently published, see Graczykowski and Lewiński (2005a). This problem has been solved under the condition of  $\sigma_T = \sigma_C$ , its generalization to the case of unequal permissible stresses being unsolved till now, see Rozvany's (1997) criticism on a part of Michell's (1904) work.

Note here that the most advanced numerical results have been recently obtained by Gilbert et al. (2005) by the truss approximation method.

The main feature of Michell trusses is their discrete-continuous structure: the mass is concentrated along the edge lines connecting the point load with the support. The lines where the mass is concentrated are interpreted as bars, i.e. usual bars of finite cross sections. They are subjected to tension or compression. Optimization removes bending and transverse shearing. The volume of the optimum structure is a sum of the volume occupied by the material forming the bars and the volume of fibres in the interior part. In the present paper we consider Michell cantilevers supported along a straight segment, lying inside a domain bounded by half-lines starting from the ends of the segment. The results of the papers by Lewiński et al. (1994) can be generalized to the case of unequal permissible local stresses, cf. Graczykowski and Lewiński (2005b). Our aim here is to consider average stresses within such optimal cantilevers, perform the local and global analyses of equilibrium. Other cases of position of the point load are discussed in Graczykowski and Lewiński (2006).

## 2. STRESS FIELDS WITHIN PRAGER–HILL CANTILEVERS

We tackle the problem of transmitting the force  $P$  applied at point  $P$  to the support  $RN$  by a plane structure lying within the infinite domain bounded by the half-lines  $RR_1$  and  $NN_1$  and by  $RN$ , cf. Figure 1. The axial stress  $\sigma$  should be bounded:  $-\sigma_C \leq \sigma \leq \sigma_T$ . The aim is to find the lightest structure satisfying the above conditions. A graphical solutions to this problem were sketched by Prager (1959) and Rozvany (1997). The analytical construction of the net of fibres within  $ABDC$  and the relevant virtual displacement fields satisfying the desired optimality conditions:

$$\bar{\varepsilon}_I = 1, \quad \bar{\varepsilon}_{II} = -\kappa \quad (1)$$

with  $\kappa = \sigma_T/\sigma_C$ , were published recently, see Graczykowski and Lewiński (2005b). Let us recall that if  $\angle NRA = \gamma_2$ ,  $\angle RNA = \gamma_1$ , we have  $\tan\gamma_1 = \kappa^{1/2}$  and  $\tan\gamma_2 = \kappa^{-1/2}$ . Thus  $r_2 = \kappa^{1/2}r_1$ , where  $r_1 = |NA|$ ,  $r_2 = |RA|$ . see Rozvany (1997). We introduce notation:  $\theta_1 = \angle ANC$ ,  $\theta_2 = \angle BRA$ . The circular domains  $BRA$ ,  $ANC$  are called fans; they are filled up with infinitely thin radial bars, called fibres. The boundary bars  $RB$  and  $NC$  have finite cross sections – they are typical truss members. The domain  $ABDC$  is parameterized with a special curvilinear system  $(\alpha, \beta)$ . The units of  $\alpha$  and  $\beta$  are radians. The vertices of  $ABDC$  have the coordinates:  $A(0, 0)$ ,  $B(0, \theta_2)$ ,  $C(\theta_1, 0)$ ,  $D(\theta_1, \theta_2)$ . This system is orthogonal; its Lamé coefficients  $A(\alpha, \beta)$ ,  $B(\alpha, \beta)$  are also radii of curvatures of the parametric lines. The parametric lines  $(\alpha, \beta)$  are determined by Cartesian coordinates  $x(\alpha, \beta)$ ,  $y(\alpha, \beta)$  measured along the  $(x, y)$  axes, as in Figure 1.

The formulae for  $x(\alpha, \beta)$ ,  $y(\alpha, \beta)$ ,  $A(\alpha, \beta)$ ,  $B(\alpha, \beta)$  were published in Graczykowski and Lewiński (2005b). Let us mention only that the Hencky net in  $ABDC$  is characterized by  $\phi(\alpha, \beta) = \beta - \alpha$ ; here  $\phi$  represents an angle between a tangent to the  $\alpha$ -line at point  $(\alpha, \beta)$  and the  $x$  axis, see Hemp (1973), where this notation is explained in detail.

The conditions (1) determine the virtual displacement field  $\bar{u} = (u, v)$ ;  $u$  and  $v$  represent displacements along  $\alpha$  and  $\beta$  lines. The integration technique explained in Hemp (1973) makes it possible to find the integral formula for  $u(\alpha, \beta)$  and  $v(\alpha, \beta)$ . However, to make these formulae useful for further analysis of longer cantilevers one should put them in terms of known special functions. It turns out that the functions introduced by Chan (1975, Appendix) and named  $G_n(\alpha, \beta)$ ,  $F_n(\alpha, \beta)$  in Lewiński et al. (1994) suffice to express all the unknowns explicitly, not only  $A$ ,  $B$ ,  $u$ ,  $v$  within  $ABDC$  but also their extensions as well as stress fields.

These functions satisfy the hyperbolic equation  $LH_n = 0$ , where  $H = G$  or  $F$  and  $L = \frac{\partial^2}{\partial\alpha\partial\beta} - 1$ . Just this equation governs the behavior of Lamé coeffi-

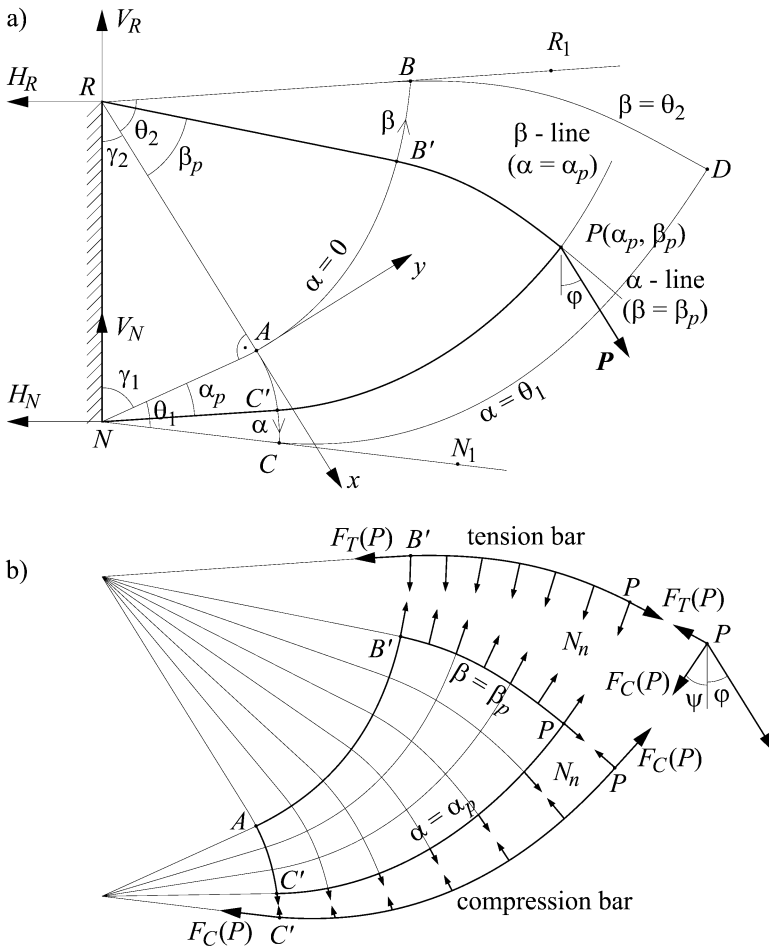


Figure 1. Prager-Hill cantilever. The feasible domain is determined by  $RN$  and the angles  $\angle R_1RN$ ,  $\angle N_1NR$ .

icients, rotated coordinate functions  $\bar{x}$ ,  $\bar{y}$  defined by  $\bar{x} + i\bar{y} = \exp(-i\phi)(x + iy)$  as well as the auxiliary displacement fields

$$\begin{aligned} u^0(\alpha, \beta) &= u(\alpha, \beta) - (\kappa + 1)\alpha A(\alpha, \beta), \\ v^0(\alpha, \beta) &= v(\alpha, \beta) + (\kappa + 1)\beta B(\alpha, \beta). \end{aligned} \tag{2}$$

In the present paper we show that the force fields associated with the Hencky net of the  $ABDC$  domain, caused by a point load  $P$  at point  $P = P(\alpha_p, \beta_p)$ , lying within  $ABDC$ , can also be expressed in terms of Chan's functions  $G_n$ . The optimal cantilever occupies the domain  $RB'PC'N$ , see Figure 1. Having found the force fields we can compute the volume by direct integration over the

fibrous domains  $RB'A$ ,  $NAC'$  and  $AB'PC'$  and along the lines of reinforcing bars  $RB'P$  and  $NC'P$ . It turns out that the volume computed this manner confirms the correctness of the whole solution. The problem of finding force fields in the cantilever of Figure 1 has never been discussed till now.

We shall use notation of a classical plate theory. The average stress resultants referred to the  $(\alpha, \beta)$  system will be denoted by  $N_I$ ,  $N_{II}$  since  $\alpha$  and  $\beta$  lines are lines of principal directions of tensor  $\mathbf{N}$ . We do not use notation:  $\sigma_I$ ,  $\sigma_{II}$  to distinguish between average and local stresses. Let us recall that the differential equations of equilibrium referred to the  $(\alpha, \beta)$  system have here the form

$$-\frac{\partial(BN_I)}{\partial\alpha} + \frac{\partial B}{\partial\alpha}N_{II} = 0, \quad -\frac{\partial(AN_{II})}{\partial\beta} + \frac{\partial A}{\partial\beta}N_I = 0. \quad (3)$$

These equations are identical with the first two differential equations of membranes parameterized by an orthogonal curvilinear system. It is Hemp (1973) who discovered that equations (3) can be simplified by changing the unknowns  $T_1 = BN_I$ ,  $T_2 = AN_{II}$ . By using the differential constraints linking  $A$  and  $B$  we reduce (3) to the form

$$T_2 = \frac{\partial T_1}{\partial\alpha}, \quad T_1 = \frac{\partial T_2}{\partial\beta} \quad (4)$$

not involving Lamé coefficients. Thus we see that  $LT_1 = 0$ ,  $LT_2 = 0$ , which makes it possible to apply the Riemann method, already used for finding the Hencky net  $(\alpha, \beta)$ . Note that  $T_1, T_2$  are of force dimension. They measure the forces per unit angles and not per unit lengths. From mechanics point of view these fields have similar meaning to axial forces in truss members. If we put (4) in the variational form

$$\iint \left[ T_1 \left( \frac{\partial \bar{u}}{\partial \alpha} + \bar{v} \right) + T_2 \left( \frac{\partial \bar{v}}{\partial \beta} + \bar{u} \right) \right] d\alpha d\beta = \int_{\alpha=\text{const}} \hat{T}_1 \bar{u} d\beta + \int_{\beta=\text{const}} \hat{T}_2 \bar{v} d\alpha \quad (5)$$

for all kinematically admissible  $\bar{u}, \bar{v}$  we note that (5) can be discretized to the variational equilibrium equation of a truss. Here  $\hat{T}_1$  ( $\hat{T}_2$ ) are given loadings normal to the edges  $\alpha = \text{const}$  ( $\beta = \text{const}$ ). We write (5) symbolically as

$$\iint T_1 d\beta(d\bar{u} + \bar{v}d\alpha) + \iint T_2 d\alpha(d\bar{v} + \bar{u}d\beta) = \bar{L}_{\text{ext}}, \quad (6)$$

where  $\bar{L}_{\text{ext}}$  represents the virtual work of given loading. Note that

$$d\bar{u} + \bar{v}d\alpha = (A d\alpha)\bar{e}_I, \quad d\bar{v} + \bar{u}d\beta = (B d\beta)\bar{e}_{II} \quad (7)$$

represent elongations of  $\alpha$  and  $\beta$  fibres of lengths  $A d\alpha$  and  $B d\beta$ , respectively. We remember that  $T_1 d\beta$  is a longitudinal force in the strip of width  $B d\beta$  along

the  $\alpha$ -line and  $T_2 d\alpha$  is such a force in the strip of width  $A d\alpha$  along the  $\beta$ -line. The associated elongations of these strips are  $\bar{\Delta}_\alpha = A d\alpha \bar{\varepsilon}_I$ ,  $\bar{\Delta}_\beta = B d\beta \bar{\varepsilon}_{II}$ . Let us imagine that the Hencky net  $(\alpha, \beta)$  is replaced by a net of finite number of  $\alpha$  and  $\beta$  lines constructed from straight segments, treated further as members of a certain truss. We imagine that the forces  $T_1 d\beta$  and  $T_2 d\alpha$  are now concentrated along the members. These forces are now treated as axial forces  $Z_K^\alpha, Z_L^\beta$  in the truss; here  $K, L$  index the members. They do a virtual work on elongations  $\bar{\Delta}_\alpha^K$  and  $\bar{\Delta}_\beta^L$ . Thus Equation (6) is replaced with

$$\sum_K Z_K^\alpha \bar{\Delta}_\alpha^K + \sum_L Z_L^\beta \bar{\Delta}_\beta^L = \bar{L}_{\text{ext}} \quad (8)$$

and if the independent virtual displacements of nodes are denoted by  $\bar{q}_1, \dots, \bar{q}_s$ , then  $\bar{L}_{\text{ext}}$  is replaced by  $\bar{\mathbf{q}}^T \mathbf{Q}$  with  $\mathbf{Q}$  being the vector of effective nodal forces. To note that (8) represents equations of nodes of the approximating truss we should put  $Z_K^\alpha, Z_L^\beta$  into one column  $\mathbf{Z}$ , put elongations  $\bar{\Delta}_\alpha^K, \bar{\Delta}_\beta^L$  into one column  $\bar{\mathbf{\Delta}}$  and correlate them with nodal virtual displacements by linear equations:  $\bar{\mathbf{\Delta}} = \mathbf{B}\bar{\mathbf{q}}$ ,  $\mathbf{B}$  being a geometry matrix. Thus Equation (8) implies  $\bar{\mathbf{\Delta}}^T \mathbf{Z} = \bar{\mathbf{q}}^T \mathbf{Q}$  hence  $\mathbf{B}^T \mathbf{Z} = \mathbf{Q}$ , because  $\bar{\mathbf{q}}$  is arbitrary. We conclude that Equation (6) can be approximated by truss equilibrium equations, with arbitrary accuracy.

Let us come back to the problem of equilibrium of the cantilever of Figure 1. We should decompose it into two reinforcing bars  $B'P$  (in tension,  $F_T > 0$ ) and  $C'P$  (in compression,  $F_C < 0$ ), the node  $P$  subjected to three forces of magnitudes:  $F_T(P), F_C(P), P$ , the fibrous domain  $B'PC'A$ , the fans  $RB'A, NAC'$  with edge bars  $RB', NC'$  and the rectangle  $RAN$  is empty. Kinematic consideration starts from  $RAN$  domain and moves to the right. On the contrary, static analysis starts from equilibrium of node  $P$  and moves left. The net is already found (see Graczykowski and Lewiński (2005b)) so we know the angle  $\psi$  between tangent to  $C'P$  at  $P$  and the vertical line  $RN$ :  $\psi = \gamma_1 + \alpha_p - \beta_p$ . Angle  $\varphi$  is directed counterclockwise, see Figure 1a.

Note first that the longitudinal forces  $F_T$  and  $F_C$  do not vary along  $B'P$  and  $C'P$ , since no tangent loading is applied. Thus  $F_T = F_T(P)$  and  $F_C = F_C(P)$ . The magnitudes of forces  $F_T(P), F_C(P)$  found from equilibrium equations of node  $P$

$$F_C(P) = -P \cos(\psi + \varphi), \quad F_T(P) = P \sin(\psi + \varphi) \quad (9)$$

determine the longitudinal forces in the bars  $B'P$  and  $C'P$ . Since  $B'R$  ( $C'N$ ) is a smooth extension of  $B'P$  ( $C'P$ ) at  $B'$  ( $C'$ ) the axial forces in  $RB'$  (and  $NC'$ ) are still equal to  $F_T(P)$  (and  $F_C(P)$ ). Note that the bar  $RB'P$  works like a cord, since it slides along  $B'P$ . The bar  $PC'$  is compressed with no buckling allowed. The equilibrium equations of both the bars determine the magnitude

of the normal loading  $N_n$ . Since Lamé coefficients are equal here to the radii of curvatures we obtain

$$N_n = -F_C(P) \quad \text{for } \alpha = \alpha_p, \quad N_n = -F_T(P) \quad \text{for } \beta = \beta_p, \quad (10)$$

see Figure 1b. These formulae provide the boundary conditions

$$T_1(\alpha_p, \beta) = -F_C(P), \quad T_2(\alpha, \beta_p) = -F_T(P) \quad (11)$$

We can apply now Riemann's method, as explained in Lewiński et al. (1994, equation (17)) and find

$$\begin{aligned} T_1(\alpha, \beta) &= -F_C G_0(\alpha_p - \alpha, \beta_p - \beta) + F_T G_1(\alpha_p - \alpha, \beta_p - \beta), \\ T_2(\alpha, \beta) &= -F_T G_0(\alpha_p - \alpha, \beta_p - \beta) + F_C G_1(\beta_p - \beta, \alpha_p - \alpha). \end{aligned} \quad (12)$$

Having found  $T_1, T_2$  we can compute their boundary values along  $AB'$  and  $AC'$ , which determines force fields within the circular fans  $RB'A, NAC'$ . It occurs that the circumferential stresses vanish and the radial stresses are constant along the radii. Now we know the force fields  $T_1, T_2$  within the whole structure and we know the axial forces in the ribs. The last step is to compute the reactions:  $H_R, V_R, H_N, V_N$  by considering equilibrium conditions of nodes  $R$  and  $N$ . The concentrated forces at  $R, N$  and  $P$  should give zero total vector and zero total moment around an arbitrary point (say,  $P$ ). These three algebraic equations should confirm that the whole static analysis has been done correctly.

### 3. EQUIVALENCE OF TWO FORMULAE FOR THE WEIGHT OF THE OPTIMAL PRAGER-HILL CANTILEVER

Virtual work of the force  $P$  determines the volume of the optimal cantilever:

$$\mathcal{V} = \frac{P}{\sigma_T} [u(P) \sin(\varphi + \psi) - v(P) \cos(\varphi + \psi)], \quad (13)$$

where  $P = P(\alpha_p, \beta_p)$ ; the functions  $u, v$  being given in section 9 of Graczykowski and Lewiński (2005b). Both the fields  $u$  and  $v$  are expressed in terms of Chan functions. To be sure that this result is correct we shall compute this volume directly by summing up the volumes of all the parts of the structure. Density of fibres within  $AB'PC'$  is given by

$$h(\alpha, \beta) = \frac{T_1(\alpha, \beta)}{\sigma_T B(\alpha, \beta)} - \frac{T_2(\alpha, \beta)}{\sigma_C A(\alpha, \beta)}. \quad (14)$$

We know that  $T_2 < 0$ . For the  $NAC'$  fan the formula for density  $h$  does not contain the first term. For the  $RB'A$  fan the function  $h$  is expressed by the first

term. To compute the integral

$$\mathcal{V}_{AB'PC'} = \int_0^{\alpha_p} \int_0^{\beta_p} h(\alpha, \beta) A(\alpha, \beta) B(\alpha, \beta) d\alpha d\beta, \quad (15)$$

with  $h$  being given by (14),  $T_1$ ,  $T_2$  given by (12) and  $A$ ,  $B$  given by (4) in Graczykowski and Lewiński (2005b) one should apply the integration rules (31)–(36) of Lewiński et al. (1994).

The expressions for  $\mathcal{V}_{NAC'}$  and  $\mathcal{V}_{RB'A}$  can be found by similar integration. Now we compute the volume of the tension ( $T$ ) bar

$$\mathcal{V}_T = \frac{F_T(P)}{\sigma_T} \left( \int_0^{\alpha_p} A(\alpha, \beta_p) d\alpha + r_2 \right). \quad (16)$$

The formula for the volume  $\mathcal{V}_c$  of the compression bar is similar.

This integration can be performed by using properties of Chan's functions. By summing up the volumes of material used for construction of fibrous domains  $AB'PC'$ ,  $NAC'$ ,  $RB'A$  and of the ribs  $RB'P$ ,  $NC'P$  we arrive at  $\mathcal{V}$  coinciding exactly with formula (13). We say that the duality gap between the dual and primal formulations vanishes.

#### 4. FAMILY OF CANTILEVERS DESIGNED WITHIN A STRIP. BENCHMARK RESULTS

Let us consider the case of  $\kappa = 3$ ,  $\theta_1 = \pi/6$ ,  $\theta_2 = \pi/3$ . Then the feasible domain is a strip, see Figure 2. The force  $P$  is assumed to act parallel to the  $RN$  supporting line, or  $\varphi = 0$ , its application point  $P$  being on the midperpendicular to  $RN$  at a distance  $d$  from  $RN$ . Let  $\xi = d/a$ , with  $a = |RN|$ . Thus the family of problems is indexed by  $\xi$ . If  $\xi = \sqrt{2}/2$  the optimal structure is composed of two bars and one circular fan. If  $\xi > \sqrt{2}/2$ , point  $P$  lies at the right side of  $P_0$ , where  $|RP_0| = |RA| = a\sqrt{3}/2$ ,  $|RO| = a/2$ . Let the volume of the optimal cantilever be denoted by  $\mathcal{V}$  and its non-dimensional counterpart by  $\bar{\mathcal{V}} = \mathcal{V}/(Pa/\sigma_T)$ . The values of  $\bar{\mathcal{V}}$  are set up in Table 1 for subsequent values of the distance  $d = \xi a$  of the force  $P$  to the  $RN$  line. The same table gives also the curvilinear coordinates  $(\alpha_p, \beta_p)$  of subsequent position of point  $P$ .

The midperpendicular of  $RN$  crosses subsequent domains of kinematic division, as introduced in Graczykowski and Lewiński (2005b, 2006). Thus the graph of the volume of Figure 3 refers not to one but to several types of the cantilevers: for  $0 \leq \xi \leq \sqrt{3}/6$  the optimal structure is composed of two bars; for  $\sqrt{3}/6 \leq \xi \leq \sqrt{2}/2$  the optimal structure is composed of one circular fan and two bars; for  $\sqrt{2}/2 \leq \xi \leq 1.522008$  the solution is called Prager–Hill cantilever; for  $1.522008 \leq \xi \leq 2.036580$  the solution includes additionally one Chan-like domain; for  $2.036580 \leq \xi \leq 3.028582$  the solution includes two Chan-like domains and one Hill-like domain more.



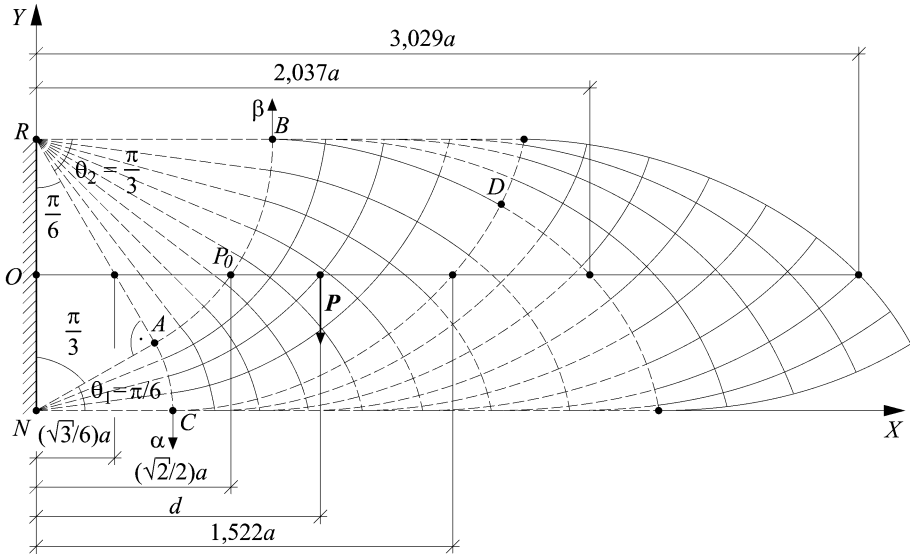


Figure 2. Case of:  $\kappa = 3$ ,  $\theta_1 = \pi/6$ ,  $\theta_2 = \pi/3$ ,  $\varphi = 0$ . Chan's domains are indicated by dashed lines.

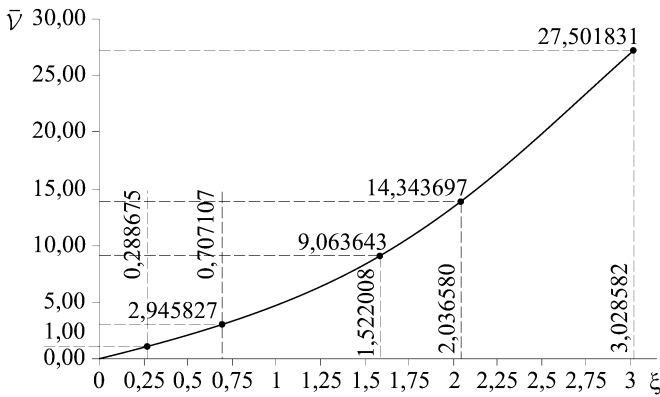


Figure 3. Non-dimensional volume  $\bar{V}$  of the optimal cantilevers.

Nonetheless, the graph of the volume versus  $\xi$  is smooth, even at points  $\xi = \sqrt{3}/6$ ,  $\sqrt{2}/2$ , 1,522008, 2,036580, 3,028582, where the structure of the solution switches to a more complicated form.

The results set up in Table 1 are benchmark results for possible numerical checks based on a ground structure method or other numerical-oriented basis.

Table 1. Non-dimensional volume  $\bar{V}$  of the optimal cantilevers.

$\xi$	$\alpha_p$	$\beta_p$	$\bar{V}$
0	–	–	0
0.25	–	–	0.86602540
0.5	–	0.26179939	1.88962418
0.75	0.03909955	0.45996378	3.18119647
1	0.23418873	0.61048885	4.77413280
1.25	0.38788355	0.73867388	6.68710224
1.5	0.51357763	0.84847879	8.86123302
1.75	0.66391239	0.94562854	11.27758404
2	0.80344224	1.03477767	13.93605154
2.25	0.93237717	1.16472612	16.83306684
2.5	1.05679215	1.29767843	19.99191059
2.75	1.17798254	1.42731919	23.40492241
3	1.29752093	1.55600661	27.06729757

## 5. FINAL REMARKS

Construction of Hencky nets within the trapezoidal domains, as outlined in Graczykowski and Lewiński (2005b), is complemented here by the analysis of force fields within the fibrous domains and in the reinforcing ribs. The force fields and Lamé fields determine the density of fibers as well as the cross sections of the ribs. Integration of the mass density confirms the values of the volumes of the optimal cantilevers found previously by the Michell-like kinematic formulae.

## REFERENCES

- Chan, H.S.Y. (1967) Half-plane slip-line fields and Michell structures, *Q. J. Mech. Appl. Math.*, 20, 453–469.
- Chan, H.S.Y. (1975) Symmetric plane frameworks of least weight, in *Optimization in Structural Design*, A. Sawczuk and Z. Mróz, (eds), Springer-Verlag, Berlin, pp. 313–326.
- Gilbert, M., Darwich, W., Tyas, A. and Shepherd, P. (2005) Application of large-scale layout optimization techniques in structural engineering practice, in *6th World Congress of Structural and Multidisciplinary Optimization*, Rio de Janeiro, 30 May–3 June 2005, Brasil, CD ROM, in press.
- Golay, F. and Seppecher, P. (2001) Locking materials and the topology of optimal shapes, *Eur. J. Mech. A/Solids*, 20, 631–644.
- Graczykowski, C. and Lewiński, T. (2005a) The lightest plane structures of a bounded stress level, transmitting a point load to a circular support, *Control and Cybernetics*, 34, 227–253.
- Graczykowski, C. and Lewiński, T. (2005b) New designs of Michell-like cantilevers corresponding to different allowable tensile and compressive stresses, in *6th World Congress of Structural and Multidisciplinary Optimization*, Rio de Janeiro, 30 May–3 June 2005, Brazil, CD ROM, in press.

- Graczykowski, C. and Lewiński, T. (2006) Michell cantilevers constructed within trapezoidal domains – Part I: Geometry of Hencky nets, Part II: Virtual displacement fields, Part III: Force fields, Part IV: Complete exact solutions of selected optimal designs and their approximations by trusses of finite number of joints, *Struct. Multidisc. Optimiz.*, in press.
- Hemp, W.S. (1973) *Optimum Structures*, Clarendon Press, Oxford.
- Lewiński, T. and Telega, J.J. (2001) Michell-like grillages and structures with locking, *Arch. Mech.*, 53, 303–331.
- Lewiński, T., Zhou, M. and Rozvany, G.I.N. (1994) Extended exact solutions for least-weight truss layouts – Part I: Cantilever with a horizontal axis of symmetry, Part II: Unsymmetric cantilevers, *Int. J. Mech. Sci.*, 36, 375–398, 399–419.
- Michell, A.G.M. (1904) The limits of economy of material in frame-structures, *Phil. Mag.*, 8, 589–597.
- Prager, W. (1959) On a problem of optimal design, in *Proc. IUTAM Symp. on Non-Homogeneity in Elasticity and Plasticity*, W. Olszak (ed.), Pergamon Press, London, pp. 125–132.
- Rozvany, G.I.N. (1997) Some shortcomings in Michell's truss theory, *Struct. Optimiz.*, 12, 244–250.
- Strang, G. and Kohn, R.V. (1983) Hencky–Prandtl nets and constrained Michell trusses, *Comp. Meth. Appl. Mech. Eng.*, 36, 207–222.